

三次元微細構造解析による異なる膨張原因により生じるコンクリートの損傷に関する検討

Mesoscopic analysis of different expansion causes in concrete by 3D Rigid Body Spring Model

リヤント エディ*・アヌパム アワスチ*・松本 浩嗣*・長井 宏平*・浅本 晋吾**
Liyanto EDDY, Anupam AWASTHI, Koji MATSUMOTO, Kohei NAGAI and Shingo ASAMOTO

1. INTRODUCTION

Scanning electron microscope (SEM) was used to identify the cause of the expansion in pre-tensioned pre-stressed concrete sleepers in many areas of Indian Railways¹⁾. However, it is difficult to identify whether the expansion is caused by delayed ettringite formation (DEF) or alkali silica reaction (ASR) because typical cracking patterns for both cases are similar as shown in Fig. 1 and Fig. 2, respectively.

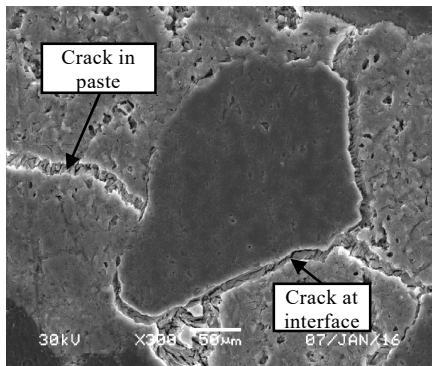


Figure 1 Typical cracking pattern of DEF

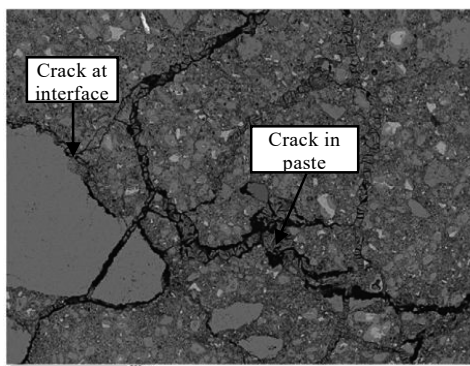


Figure 2 Typical cracking pattern of ASR²⁾

Cracks occur not only in the paste but also at the mortar-aggregate interfaces. Numerical simulation at meso-scale level where cracks are simulated directly can be a beneficial tool for understanding internal stresses and cracking conditions in concrete due to these different expansion causes. In this study, a three-dimensional discrete model, specifically the three-dimensional rigid body spring model (3D RBSM) is conducted for this purpose. In this mesoscopic analysis, mortar is modeled using elements with a size of 2-3 mm and 3D shape of aggregates is modeled directly. In our research group, 3D RBSM was conducted for the quantitative evaluation of concrete behavior by directly modeling the shape of aggregates³⁾. Thus, the objective of this research is to investigate the internal stresses and cracking conditions in concrete due to the different expansion causes using numerical simulation.

2. ANALYSIS METHOD

In this study, simulations are carried out by 3D RBSM, as proposed by Kawai et al.⁴⁾. A three-dimensional concrete model is formed from a meshed of rigid bodies. Each rigid body has six degrees of freedom, consisting of three translational degrees of freedom and three rotational degrees of freedom around certain points within its interior. Each is connected to other rigid bodies by three springs which are two shear springs and one normal spring illustrated in Fig. 3. To model the concrete in 3D, two types of elements which are mortar and aggregates are used. As the propagation of cracks in concrete is one of the most important factors affecting the behavior, the mesh arrangement in the model in RBSM is important. Voronoi diagram is used for element meshing in order to prevent crack propagating in a non-arbitrary direction. Mortar elements are modeled with a size of approximately $2 \times 2 \times 2-3 \times 3 \times 3$ mm³ and 3D shape of aggregates is modeled directly where a circular or sphere shape is used for representing aggregate in 3D. The meso-scale mesh arrangement used for mortar and aggregates in this study is presented in Fig. 4. The properties of the springs are determined such that the

*Institute of Industrial Science, The University of Tokyo, Japan

**Department of Civil & Environmental Engineering, Saitama University, Japan

研究速報

elements, when combined together, are able to predict accurately the response determined in laboratory scale material test. The simulation system and constitutive models developed by Nagai et al.³⁾ are used.

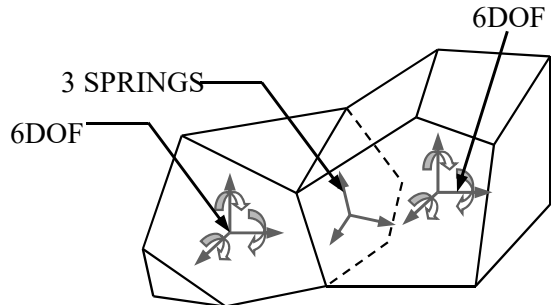


Figure 3 3D RBSM mechanical model

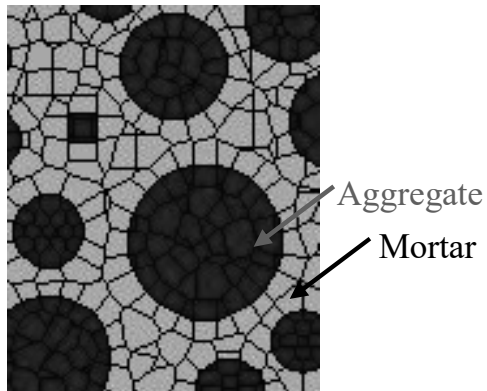


Figure 4 Mesh arrangement for mortar and aggregates

3. ANALYSIS METHOD

3.1 Geometry of Numerical Models

Fig. 5 shows an analyzed numerical model. The size of the model is 150×150×150 mm. Aggregate size distribution is determined based on the JSCE Standard Specification for Concrete Structures⁵⁾ and the maximum aggregate size is 20 mm as shown in Fig. 6. Aggregate diameters used for the analysis are varied with 2 mm increments. The number of aggregates of each size is calculated using the distribution curve in Fig. 6 and the points on the curve indicate the selected diameter. For the simplification purpose, the aggregates with diameter lower than 6 mm are eliminated. Target aggregate volume is approximately 30% and it becomes around 26% in the simulation. Table 1 shows the number of each aggregate and total number of aggregates.

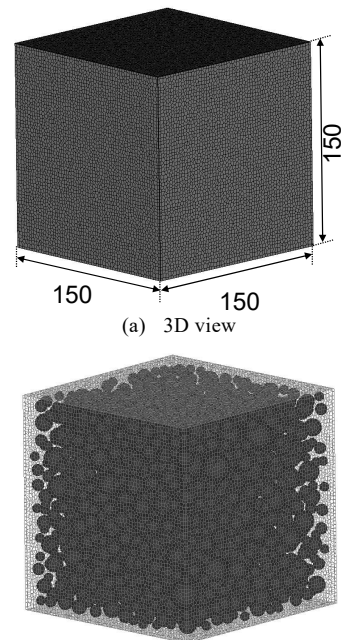


Figure 5 3D concrete model (units: mm)

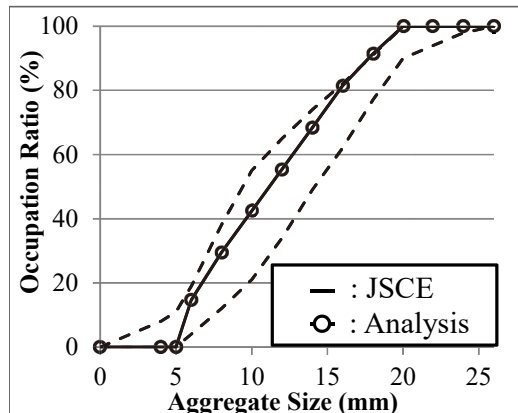


Figure 6 Grain size distributions

Table 1 Introduced aggregates

Aggregate size (mm)	Amount
6	1316
8	555
10	251
12	145
14	92
16	61
18	33
20	21

3.2 Numerical Models

Six cases are simulated which are listed in Table 2 and illustrated in Fig. 7. The expansion in concrete is applied by the concept of expansion strain (Matsumoto et al.⁶⁾). In the case of

DEF-type, to represent the paste expansion, the expansion strain is applied in the mortar. Three numerical models, named by DEF100, DEF50, and DEF25, are considered in this case. DEF100 means that all springs between mortar elements expand. DEF50 means that 50% of all springs between mortar elements (randomly selected) expand. DEF25 means that 25% of all springs between mortar elements (randomly selected) expand. Meanwhile, in the case of ASR-type, the expansion strain is applied at the mortar-aggregate interfaces to reflect the expansion due to the alkali silicate gel product formed in the aggregates. Three numerical models, named by ASR100, ASR50, and ASR25, are also considered in this case. ASR100 means that all mortar-aggregate interfaces expand. ASR50 means 50% of all mortar-aggregate interfaces (randomly selected aggregates) expand,

while ASR25 means that 25% of all mortar-aggregate interfaces (randomly selected aggregates) expand.

The material properties for the mortar, aggregates, and mortar-aggregate interfaces are also listed in Table 2. In order to obtain the same volume expansion of concrete at each loading step, with less percentage of locations of the expansion, the expansion strain is higher at each strain-inducing step. Expansion strain is increased by 600 microns in cases DEF100 and ASR100, 1200 microns in cases DEF50 and ASR50, and 2400 microns in cases DEF25 and ASR25 at each step. 150 steps of expansion strain-inducing are applied in the simulation.

4. RESULTS AND DISCUSSIONS

4.1 Surface Cracks

A 3D representation of the surface cracks for all simulation models is shown in Fig. 8. Simulation results show that cracking pattern on the concrete surface depends on the expansion cause in the concrete. The cracks are distributed on the concrete surface when the expansion occurs in the mortar (DEF100, DEF50, and DEF25). Furthermore, with less percentage of locations of the expansion, the cracking pattern does not change. Meanwhile, when the expansion occurs at the mortar-aggregate interfaces, map cracks are predicted on the concrete surface (ASR100, ASR50, and ASR25). With less percentage of locations of the expansion, cracks on the concrete surface become more localized.

4.2 Internal Cracks and Stresses

By studying the internal stresses and cracks in the simulation results, the cause of the difference in the cracking pattern on the concrete surface is investigated.

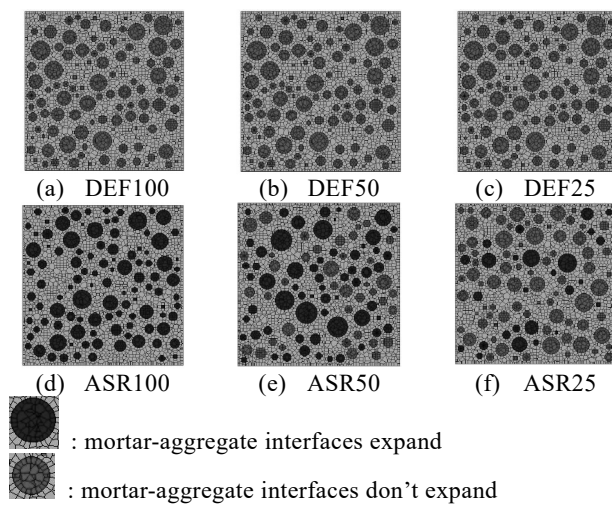


Figure 7 Simulation cases

Table 2 Model details

Case	Parameter	Number of elements	Mortar			Aggregate	Interface
			Modulus of elasticity E_c (MPa)	Tensile strength f_t (MPa)	Compressive Strength f'_c (MPa)		
DEF100	All springs between mortar elements expand	211,785	33,000	3,121	50	50,000	1.79
DEF50	50% of all springs between mortar elements expand	211,785					
DEF25	25% of All springs between mortar elements expand	211,785					
ASR100	All mortar-aggregate interface expand	211,691					
ASR50	50% of all mortar-aggregate interface expand	211,730					
ASR25	25% of all mortar-aggregate interface expand	212,753					

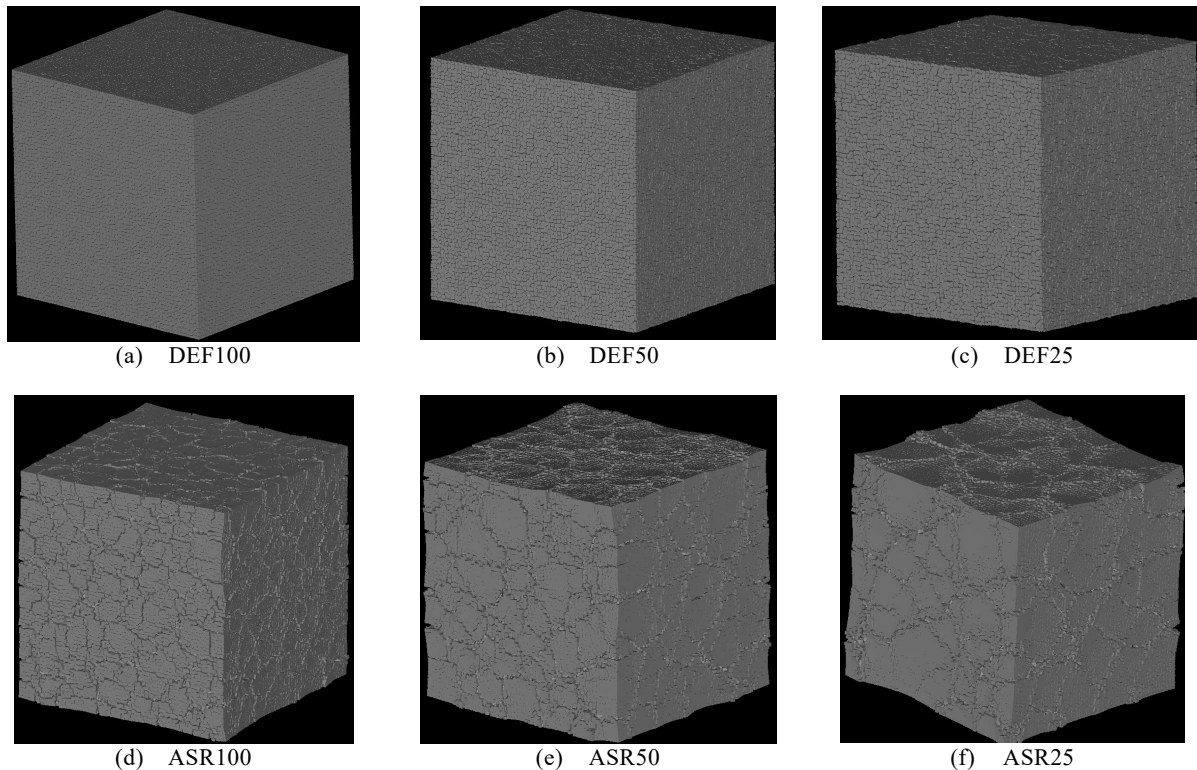
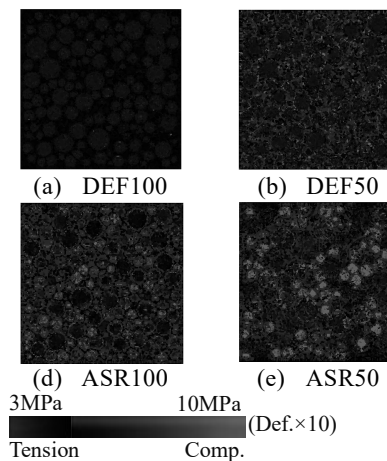
Figure 8 Surface cracks (deformation $\times 10$)

Figure 9 Internal stresses and cracks for all cases at a volume expansion of 0.01%

Fig. 9 shows the internal stress and crack distributions of x-y cross section at $z = 75$ mm, when the volume expansion of concrete is 0.01%. These internal stress distributions show that at early expansion, there are different stress distributions in the concrete depending on the expansion cause. In the DEF-type cases, tensile stresses are formed in the aggregates. With less percentage of locations of the mortar expansion, the compressive and tensile stresses are more distributed in the mortar. Meanwhile, in the ASR-type cases, compressive stresses are formed in the

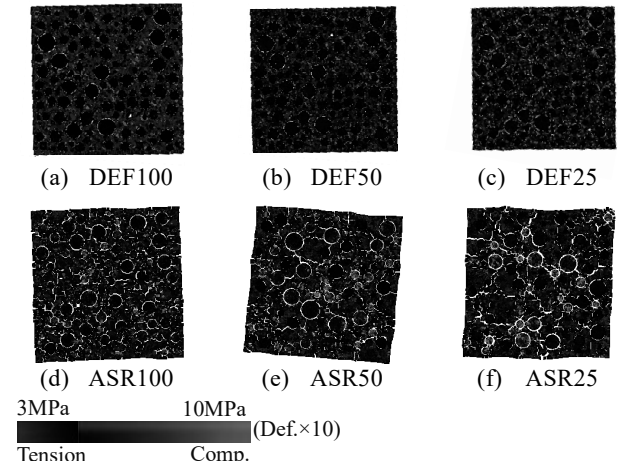


Figure 10 Internal stresses and cracks for all cases at a volume expansion of 1%

aggregates. With less percentage of locations of the mortar-aggregate interface expansion, tensile stresses are more localized in the mortar.

Fig. 10 shows the internal stress and crack distributions of x-y cross section at $z = 75$ mm, when the volume expansion of concrete is 1.00%. As the expansion increases, the internal stress distributions change in both cases (ASR-type cases and DEF-type cases). In the DEF-type cases, there is no stress formed in the aggregates because cracks occur at the mortar-aggregate

interfaces. No stress can be transferred into the aggregates and, furthermore, the compressive and tensile stresses are distributed only in the mortar. As a result, cracks are also distributed in the mortar and at mortar-aggregate interfaces.

In the ASR-type cases, stresses in the aggregates and mortar decreases because localized cracks in the mortar open. With less percentage of locations of the mortar-aggregate interface expansion, cracks become more localized. These localized cracks in the mortar and the expansion at the mortar-aggregate interfaces are connected. As a result, map cracks occur in the concrete.

Based on the simulation results, DEF-type cases do not match well with the typical map cracking pattern observed in the real concrete. Simple model that uniform expansion of paste takes place in DEF (Taylor et al.⁷⁾) could not reproduce the typical cracking pattern of DEF. In order to simulate the DEF appropriately, the simple model in this study needs to be improved because there might be more complex phenomenon occurred in the concrete.

5. CONCLUSIONS

Based on the mesoscopic analysis different expansion causes in concrete by 3D Rigid Body Spring Model, the following conclusions can be drawn.

- Different internal crack and stress distribution are predicted with different expansion causes. Distributed cracks occur in the concrete when the expansion occurs in the mortar and map cracks occur in the concrete when the mortar-aggregate

interfaces expand. With less percentage of locations of the mortar-aggregate interface expansion, cracks become more localized

- The simulated cracks in DEF-type cases do not match with the actual cracking pattern where the simplified paste expansion theory of DEF is modeled. Distributed cracks are predicted by the simulation and do not match with the map cracking pattern observed in the reality. Therefore, another complex mechanism of DEF may take place and the model in this study needs to be improved.

(Manuscript received. May 19, 2017)

REFERENCES

- Awasthi, A., et al., *Proc. 7th International Conference of Asian Concrete Federation*, Hanoi, Vietnam (2016).
- Thomas, M., et al., *Cement and Conc. Res.*, 38, (2008), pp841-847.
- Nagai, K., et al., *J. Adv. Concr. Technol.*, 3(3), (2005), pp385-402.
- Kawai, T., *Nucl. Eng. Des.*, 48, (1978), pp207-229.
- JSCE, *Standard Specification for Concrete Structures 2007 'design'*, (2007).
- Matsumoto, K., et al., *Proc. 13th International Symposium on New Technologies for Urban Safety of Mega Cities in Asia*, Yangon, Myanmar (2015).
- Taylor, H.F.W., et al., *Cement and Conc. Res.*, 31, (2001), pp683-693.

(This paper is a reprint from the Proceedings of 15th International Symposium on New Technology for Urban Safety of Mega Cities in Asia (USMCA), 2016.)